

Conducting glasses as new potential thermoelectric materials: the Cu-Ge-Te case

*António P. Gonçalves,*¹ Elsa B. Lopes,¹ Olivier Rouleau,² Claude Godart²*

¹Dep. Química, Instituto Tecnológico e Nuclear/CFMC-UL, P-2686-953 Sacavém, Portugal

²CNRS, ICMPE, CMTR, 2/8 rue Henri Dunant, 94320 Thiais, France.

apg@itn.pt, eblopes@itn.pt, rouleau@icmpe.cnrs.fr, godart@icmpe.cnrs.fr

RECEIVED DATE (to be automatically inserted after your manuscript is accepted if required according to the journal that you are submitting your paper to)

TITLE RUNNING HEAD: Conducting glasses as thermoelectric materials

CORRESPONDING AUTHOR FOOTNOTE:

António P. Gonçalves

Dep. Química, Instituto Tecnológico e Nuclear/CFMC-UL, Estrada Nacional 10, P-2686-953 Sacavém, Portugal

Telephone: +351 21 9946182

Fax: +351 21 9946185

Email: apg@itn.pt

ABSTRACT Recent approaches to improve performance of bulk thermoelectric (TE) materials show that they should have complex structures, include inclusions and impurities, possess mass fluctuations, disorder and be based on heavy elements. Glasses can own these properties. In order to identify glasses with interesting TE potential, attention should be focused on small gap semiconducting or semimetallic glasses. Chalcogenide glasses with $\text{Cu}_{x+y}\text{Ge}_{20-x}\text{Te}_{80-y}$ ($0 \leq x \leq 20$; $0 \leq y \leq 10$) compositions were prepared by melt spinning. Their powder X-ray diffraction analyses point to a short-range order analogous to $\text{Ge}_{20}\text{Te}_{80}$, with copper atoms most likely replacing germanium atoms in the GeTe_4 structural unit. It also indicates, together with the differential scanning calorimetry results, a reduction of the glass stability with the increase of copper concentration. The enhancement of copper content dramatically reduces (five orders of magnitude) the electrical resistivity, while keeping the Seebeck coefficients at large values ($\sim 400 \mu\text{V K}^{-1}$). As a consequence, a huge increase on the power factor is observed, up to a maximum value of $60 \mu\text{W/K}^2\text{m}$ for the $\text{Cu}_{27.5}\text{Ge}_{2.5}\text{Te}_{70}$ glass at $T = 300 \text{ K}$. $\text{Ge}_{20}\text{Te}_{80}$ has extremely low lattice thermal conductivity values ($\sim 0.1 \text{ W/Km}$ at 300 K), which points to relatively high ZT values for this family of glasses, and indicates $\text{Cu}_{x+y}\text{Ge}_{20-x}\text{Te}_{80-y}$ -based glasses as good candidates for obtaining high performance thermoelectric materials.

KEYWORDS: Chalcogenide glasses; conducting glasses; Seebeck coefficient.

Introduction

The research of new environment friendly energy sources and optimization of energy use have become top priority to most of modern societies. Thermoelectric materials, which are able to directly convert thermal into electrical energy (using the Seebeck effect) and, reversibly, electrical into thermal energy (using the Peltier effect), have seen renewed interest due to their potential to provide a sustainable energy solution and optimization. Moreover, the absence of greenhouse effect substances, as halogenated cooling agents, and the lack of moving parts make thermoelectric devices highly attractive and reliable (as an example, NASA Voyager systems employ thermoelectric generators working uninterruptedly for more than 30 years).

The actual commercial thermoelectric devices use materials based on PbTe, Si-Ge and, in particular, Bi₂Te₃ for near room temperature applications. However, they present low efficiencies (<10%), being crucial to discover new compounds or materials that could lead to devices with improved efficiencies. The efficiency of a thermoelectric device is mainly controlled by: (i) the adimensional figure of merit, ZT , which is given by $ZT = \alpha^2 T \sigma / \lambda$ (where T represents the absolute temperature, α is the Seebeck coefficient, and σ and λ represent the electrical and thermal conductivities, respectively) and only depends on the material; (ii) the temperature difference, ΔT , between the hot and cold junctions. The maximum value of the temperature difference depends on the characteristics of the constituent materials, in particular their thermal and chemical stability, and on the available heat and cooler sources. ZT maximization can be done via both the maximization of the numerator, $\alpha^2 \sigma$ (power factor), and the minimization of the denominator, λ . α and σ depend on the charge carriers concentration, a maximum on $\alpha^2 \sigma$ being observed for concentrations of $\sim 10^{18}$ - 10^{21} carriers/cm³, which corresponds to low gap semiconductors or semimetals. λ can be considered as a sum of two different contributions, $\lambda = \lambda_e + \lambda_L$, where λ_e represents the electronic contribution and λ_L is the contribution from the lattice vibrations (phonons). As λ_e is related with σ via the Wiedemann-Franz law, $\lambda_e = LT\sigma$ (L is the Lorentz factor), ZT maximization implies the minimization of λ_L .

At the beginning of the 90's Slack presented a new concept, "Phonon Glass Electron Crystal" (PGEC) [1], which proposes the research of compounds that conduct electricity as a crystalline material and heat as a glass. This concept has led to a better understanding of the mechanisms that affect the phonons propagation without changing significantly the electrical charge propagation and to the development of general rules to increase the thermoelectric systems performance, the most important ones being [2]: (i) use of compounds with complex crystal structures; (ii) presence of heavy atoms weakly bounded to the structures; (iii) existence of inclusions and/or impurities; (iv) formation of solid solutions; (v) existence of a large number of grain boundaries. It must be noted that these rules are not exclusive and several can exist simultaneously in the same material. As a consequence, the PGEC concept, together with the use of modern synthesis techniques, has led to the discovery of new materials with improved thermoelectric characteristics, as the skutterudites, clathrates, half-Heusler phases or low dimensional systems [3]. However, the efficiency increase of the new bulk materials is still limited to ~50% [3] and the cost of low dimensional systems is very high. Therefore, it is highly desirable to identify and study new thermoelectric systems.

The careful analysis of the main general rules to increase the thermoelectric systems performance points to conducting glasses as one of the best potential materials. Indeed, this type of materials follows almost all the main rules: they have extremely complex structures, with a certain degree of order only at small distances, can have heavy atoms weakly bounded to the structure and present mass fluctuations, easily allowing high concentrations of inclusions and impurities. In this work is described a first study on the possibility of using conducting glasses for thermoelectric applications (up to the authors best knowledge, before the present work only a theoretical paper was dedicated to this subject [4]). Preliminary experimental results already resulted on a national patent [5].

As was stressed before, to identify glasses (or any other type of materials) with improved thermoelectric performances it is necessary to center the studies on low gap semiconductor and semimetal glasses. Several glasses with semiconducting properties and containing heavy elements have already been reported in the literature, most of them based on pnictides and chalcogenides [6,7]. This

pioneer work was centered on $\text{Ge}_{20}\text{Te}_{80}$ -based glasses: the original $\text{Ge}_{20}\text{Te}_{80}$ glass is mainly formed by heavy atoms; is based only on two elements; has been described as easy to prepare [8] and it is reported as having a high Seebeck coefficient [9]; it has been also described as having small electrical conductivity values [9], but doping it with silver or copper dramatically increases its electrical conductivity [10,11]. For all these reasons we decided to study the $\text{Cu}_{x+y}\text{Ge}_{20-x}\text{Te}_{80-y}$ glasses as starting test materials and here is presented their synthesis, X-ray diffraction characterization, differential thermal analysis, thermal conductivity measurements and electrical transport (electrical resistivity and Seebeck coefficient) studies.

Experimental Section

Samples with $(x+y)\text{Cu}:(20-x)\text{Ge}:(80-y)\text{Te}$ general nominal composition (Figure 1) were prepared from the stoichiometric amounts of the elements (Cu, Goodfellow, >99.99%; Ge, Johnson Matthey, 99.999%; Te, Alfa Aesar, >99.999%). The elemental mixtures were sealed into quartz ampoules under vacuum (10^{-5} mbar) and heated at 850°C for five periods of 10 minutes each. In between these periods, the ampoules were removed from the furnace, shaken and turned upside down (while the products are still melted) in order to achieve a good homogeneity. After the last period, the 20Ge:80Te composition sample was quenched into ice water, the other samples being removed from the furnace with no extra procedure. Pieces of all samples were used as starting materials to prepare the ribbons. The pieces were put into a quartz tube with a 0.5 mm diameter nozzle, which was inserted in the stainless steel chamber containing the melt spinning system. The pieces were then melted under the protection of an argon atmosphere and injected with a pressure of 1 bar of Ar onto a copper roller rotating with a linear speed of 1.6 m/s.

The quality of the samples was checked via X-ray diffraction and differential thermal analysis measurements, together with optical microscope observations. The X-ray powder diffraction measurements were made on powders representative of the totality of the sample, at room temperature and under a dehumidified air atmosphere. The scans were performed using a Philips X'Pert

diffractometer (Bragg-Brentano assembly) with a monochromatized Cu K α radiation, a 2θ -range of 10° - 70° , a step width of 0.03° and 30 s of counting time per 2θ step. The glass transition (T_g), crystallization (T_c) and melting (T_m) temperatures of the materials were measured by differential scanning calorimetry (DSC), by using a DuPont 910 system, under an argon flux atmosphere, from 25°C to 360°C and with a constant heating rate of $10^\circ\text{C}/\text{min}$. The measurements were made using 30–40 mg of material, which was put inside an aluminum sample container; an empty aluminum container was used as reference.

Electrical resistivity and Seebeck coefficient measurements were performed in the ~ 60 - 300 K temperature range on purely glassy pieces, with a needle-like shape of $\sim 2\text{mm} \times 0.25\text{ mm}^2$, removed from each sample. A previously described cell [12], attached to the cold stage of a closed cycle cryostat, was used. The resistivity was measured by a four-probe method using the DC technique with a Keithley 220 current source and a Keithley 619 electrometer. The Seebeck coefficient was measured by a slow ac technique (ca. 10^{-2} Hz), the voltage across the sample and gold leads being measured with a Keithley 181 nanovoltmeter. The oscillating thermal gradient was kept below 1 K and was measured by a Au-0.005 at % Fe versus chromel thermocouple. The absolute Seebeck coefficient of the sample was obtained after correction for the absolute Seebeck coefficient of the gold leads (99.99% pure gold) by using the data of Huebener [13].

The thermal conductivity of the $\text{Cu}_{20}\text{Te}_{80}$ glass was measured by a standard four-contact slow ac method, relative to a constantan wire. The method used was very similar to the one previously described [14], only this time the sample and the constantan wire were thermally connected to the copper cell with the help of screws and copper plates, and glued together with silver paste. The two constantan-chromel $12\ \mu\text{m}$ diameter thermocouples were glued with GE varnish, one to the sample and the other to the constantan, and the voltages measured with two Keithley 181 nanovoltmeters. The temperature gradients used were as small as possible (typically <5 K) and the results were calculated using data taken from ref. [15].

Results and Discussion

The $\text{Cu}_{x+y}\text{Ge}_{20-x}\text{Te}_{80-y}$ glasses show X-ray diffraction patterns comparable to $\text{Ge}_{20}\text{Te}_{80}$ (Figure 2), pointing to analogous short-range order in this type of materials. The structure of $\text{Ge}_x\text{Te}_{100-x}$ ($10 \leq x \leq 25$) glasses has been extensively investigated due to their possible technological applications on optical data storage devices. The most recent X-ray diffraction studies, using high-energy synchrotron radiation, agree well with previous neutron diffraction works [16] and describe it as composed by GeTe_4 tetrahedral structural units, which are bridged by Te-Te bonds [17,18]. $\text{Cu}_{x+y}\text{Ge}_{20-x}\text{Te}_{80-y}$ glasses are much less studied, but X-ray diffraction investigations made on the $\text{Cu}_{0.08}\text{Ge}_{0.18}\text{Te}_{0.74}$ material also point out the existence of GeTe_4 tetrahedral structural units, together with other tetrahedral units centered on the copper atoms, such as CuGeTe_3 and CuTe_4 [19] (in fact, CuTe_4 tetrahedral units also exists in the CuTe compound [20] that crystallizes in its own structure -type, which supports too the possibility of having this type of unit in the $\text{Cu}_{x+y}\text{Ge}_{20-x}\text{Te}_{80-y}$ glasses). Therefore, in $\text{Cu}_{x+y}\text{Ge}_{20-x}\text{Te}_{80-y}$ glasses, the increase of the copper content, simultaneously with a large germanium and a smaller tellurium decrease (87.5% and 12.5%, respectively, in the case of higher copper concentration glass, $\text{Cu}_{27.5}\text{Ge}_{2.5}\text{Te}_{70}$), can be mainly seen as copper replacing germanium atoms in the GeTe_4 structural unit, together with the formation of some new CuTe_4 structural units.

Optical microscope observations of the samples show that they generally have a glassy aspect. However, those with higher copper concentrations frequently present regions where crystallization already appears (Figure 3). This is most probably due to: (i) a decrease of the glass stabilization with the increase of copper content; (ii) the existence of inhomogeneities on the cooling rate during the melt spinning process. These facts are also evidenced on the X-ray diffraction measurements, where many of the higher copper concentration samples already show small crystallization peaks, which can be indexed as Te and $\text{Cu}_{1.33}\text{Ge}_{0.54}\text{Te}_2$ (Figure 2). The extreme composition 30Cu:70Te, albeit still presenting some disorder, is formed by Te and CuTe , and therefore its physical properties have not been studied.

DSC measurements show a single glass transition for all compositions, albeit copper samples present more than one exothermal peak, pointing to a sequential crystallization of more than one phase (Figure 4). This can be understood by the different atomic-scale structures of the different $\text{Cu}_{x+y}\text{Ge}_{20-x}\text{Te}_{80-y}$

glasses, with the Te segregation followed by the $\text{Cu}_{1.33}\text{Ge}_{0.54}\text{Te}_2$ crystallization, similarly to what was observed in $\text{Ge}_{20-x}\text{Te}_{80-x}$ ($x = 5, 10$) glasses (Te segregation followed by GeTe crystallization) [21] and points to the existence of tellurium atoms not directly bonded to germanium or copper atoms (Te atoms connecting ATe_4 ($A = \text{Ge}, \text{Cu}$) tetrahedra). A significant decrease of the glass transition (T_g), crystallization (T_c) and melting (T_m) temperatures with the increase of copper concentration is observed, confirming the reduction of the glass stability, already indicated by the existence of crystalline regions. A maximum decrease of $\sim 50^\circ\text{C}$ is observed for the higher copper concentration glass, $\text{Cu}_{27.5}\text{Ge}_{2.5}\text{Te}_{70}$, when compared with $\text{Ge}_{20}\text{Te}_{80}$, indicating a limited temperature range of applicability of $\text{Cu}_{x+y}\text{Ge}_{20-x}\text{Te}_{80-y}$ glasses as thermoelectric materials.

The variation of the room temperature resistivity of the $\text{Cu}_{x+y}\text{Ge}_{20-x}\text{Te}_{80-y}$ glasses as a function of composition is plotted in Figure 5. A large drop of five orders of magnitude, from $\sim 3 \times 10^8$ to $2.6 \times 10^3 \mu\Omega\text{m}$, is observed on the resistivity, the lower values corresponding to glasses with higher copper and lower germanium concentrations. This drop is much higher than those previously observed for the $\text{Ag}_x\text{GeTe}_{4.7}$ ($0 \leq x \leq 1.4$) and $\text{Cu}_x\text{Ge}_{15}\text{Te}_{85-x}$ ($0 \leq x \leq 9$) glasses [10,11], probably due to the successful preparation of glasses with higher copper concentrations in the present work and to the different main type of atomic substitution. The electrical conductivity of chalcogenide glasses has been ascribed to depend on three major factors: (i) the bond strengths, (ii) the network connectivity and (iii) the density [22]. In the $\text{Cu}_{x+y}\text{Ge}_{20-x}\text{Te}_{80-y}$ glasses the main factor should be the first one (change in the bond strengths). Indeed, in the $\text{Cu}_{x+y}\text{Ge}_{20-x}\text{Te}_{80-y}$ prepared glasses it is expected that copper mainly replaces germanium in the GeTe_4 structural unit, which neither changes the network connectivity nor appreciably decreases the glass density (the density change produced by the lower atomic mass of copper should be compensated by its lower atomic volume, when compared with germanium). The formation of new CuTe_4 structural units could significantly change the network connectivity, but its increase is expected to cause a larger splitting between σ (bonding) and σ^* (antibonding) orbitals, and, consequently, should increase the electrical resistivity [22], which is not observed. On the other hand, the Cu-Te bond dissociation energy ($230.5 \pm 14.6 \text{ kJ mol}^{-1}$ [23]) is significantly smaller than the Ge-Te dissociation

energy (396.7 ± 3.3 kJ mol⁻¹ [23]), and therefore, a strong increase of the electrical conductivity is expected due to this factor [22].

All the $\text{Cu}_{x+y}\text{Ge}_{20-x}\text{Te}_{80-y}$ glasses show a semiconducting behavior, with the electrical resistivity increasing with the decreasing temperature (Figure 6). The temperature dependence of the electrical resistivity, $\rho(T)$, obeys the $\rho(T) = \rho(0) \exp(E_a/kT)$ relation, where T represents the temperature, E_a is the activation energy for the electronic conduction (half of the energy gap) and k represents the Boltzmann constant. A significant variation of the high temperature activation energy can be observed with the change of composition (Table 1), the higher and the lower values (470 meV and 126 meV) being observed for the un-substituted $\text{Ge}_{20}\text{Te}_{80}$ and with upper copper concentration glass, $\text{Cu}_{27.5}\text{Ge}_{2.5}\text{Te}_{70}$, respectively. When it was possible to measure a large enough temperature range, it was observed that the activation energy starts to slightly decrease below a certain temperature. The magnitude of the high temperature activation energies confirms the narrow-gap semiconducting character of the studied glasses, being similar to those observed on the best classical thermoelectric materials, PbTe (~100-250 meV), Si-Ge (~350-550 meV) and Bi_2Te_3 (~75-140 meV).

Albeit the fact that room temperature resistivity values of the $\text{Cu}_{x+y}\text{Ge}_{20-x}\text{Te}_{80-y}$ glasses are consistent with those expected for narrow-band-gap semiconductors, the best ones are still one order of magnitude higher than those observed on new materials with good thermoelectric properties, such as the skutterudites or half-Heusler phases [24,25].

The variation of the room temperature Seebeck coefficient of the $\text{Cu}_{x+y}\text{Ge}_{20-x}\text{Te}_{80-y}$ glasses as a function of composition is plotted in Figure 7. Although the resistivity decreases by five orders of magnitude, the increase of copper concentration has a much limited effect on the Seebeck coefficient, with all glasses presenting very large values. A decrease of ~40% from the original $\text{Ge}_{20}\text{Te}_{80}$ value ($980 \mu\text{V K}^{-1}$) is first observed after a small copper introduction in the composition, but further increase of copper to higher concentrations just slightly decreases this value, which stabilizes at $\sim 400 \mu\text{V K}^{-1}$. The variation of the Seebeck coefficient of the $\text{Cu}_{x+y}\text{Ge}_{20-x}\text{Te}_{80-y}$ glasses as a function of temperature is plotted in Figure 8. The absolute values of the Seebeck coefficients are always positive, indicating

dominant p-type conduction for all the $\text{Cu}_{x+y}\text{Ge}_{20-x}\text{Te}_{80-y}$ glasses. In glasses with higher copper concentrations, the Seebeck coefficient is only slightly dependent on the temperature, increasing with the decreasing temperature, and their values ranging from 400 to 500 $\mu\text{V K}^{-1}$; the low copper concentration glasses show a higher increase of the Seebeck coefficient with the decreasing temperature.

The combination of a very large decrease of the electrical resistivity, together with the stabilization of the Seebeck coefficients at high values, has as a consequence a dramatic increase (of five orders of magnitude) of the power factor with the increasing copper concentration (Figure 9). An exponential increase of the power factor with increasing temperature is observed, the maximum value of 60 $\mu\text{W/K}^2\text{m}$ being obtained for the $\text{Cu}_{27.5}\text{Ge}_{2.5}\text{Te}_{70}$ composition at $T = 300\text{ K}$, the higher temperature measured.

Due to the difficulty in obtaining $\text{Cu}_{x+y}\text{Ge}_{20-x}\text{Te}_{80-y}$ glasses with an appropriate shape, it was decided to measure the thermal conductivity only on $\text{Ge}_{20}\text{Te}_{80}$ and to use the obtained values for the other compositions, after correcting them with the help of the Wiedemann-Franz law. The measured thermal conductivity of $\text{Ge}_{20}\text{Te}_{80}$ is extremely low, with a value of $\sim 0.1\text{ W/Km}$ at 300 K. Due to the high difference between the thermal conductivities of the sample and the constantan wire, used as reference, the heat radiation losses are not negligible, especially at high temperatures, (but unfortunately not easy to estimate), so the true value of $\text{Ge}_{20}\text{Te}_{80}$ thermal conductivity is certainly smaller than 0.1 W/Km at 300 K. The very low thermal conductivity value of the $\text{Ge}_{20}\text{Te}_{80}$ glass is in agreement with measurements made on other chalcogenide glasses, where very low thermal conductivities were also observed [26]. These low values are most probably mutually consequence of the high disorder and of the high atomic weights of the constituents. The germanium replacement by copper is not expected to greatly change the lattice thermal conductivity of the glass, as any effect of the mean atomic weight decrease should be compensated by the lower Cu-Te bond strength, which should increase the rattling. The relatively high value of the electrical resistivity of $\text{Cu}_{x+y}\text{Ge}_{20-x}\text{Te}_{80-y}$ glasses at room temperature (Table 1) results on a low electronic contribution to their thermal conductivity: in $\text{Cu}_{27.5}\text{Ge}_{2.5}\text{Te}_{70}$, the glass with the higher electrical conductivity value, this contribution is only $\sim 3 \times 10^{-4}\text{ W/Km}$ and therefore

can be neglected. For the $\text{Cu}_{27.5}\text{Ge}_{2.5}\text{Te}_{70}$ glass, which has the higher power factor at 300 K, and considering a 0.1 W/Km value of the thermal conductivity at room temperature, a figure of merit value of $ZT = 0.19$ is obtained. Albeit not reaching the values of the best actual thermoelectric materials at 300 K, it is a relatively high ZT and definitely puts conducting glasses as a new class of materials candidate for obtaining high performance thermoelectric materials.

A deeper understanding of the nature of $\text{Cu}_{x+y}\text{Ge}_{20-x}\text{Te}_{80-y}$ glasses can give some hints on the way to optimize their properties. The Seebeck coefficient of a semiconducting chalcogenide glass can be expressed as [27]

$$\alpha = \pm k/e (E_{\alpha}/kT + A)$$

where e represents the electronic charge, E_{α} is the activation energy for the thermoelectric power, A is a constant that depends on the mechanism of the electrical transport, and the positive and negative signs represent the p- and n-type conduction mechanism, respectively. The observed positive Seebeck coefficient at high temperatures is very common in chalcogenide glasses, being consistent with an intrinsic conduction: if we suppose that we have an intrinsic semiconductor, the positive Seebeck coefficient is a consequence of the holes mobility being much higher than the electrons mobility in that temperature region. The activation energies obtained by fitting the data using this expression [27] at high temperatures, E_{α} , are considerably smaller than the activation energies obtained from the resistivity data (Table 1). This large difference observed in the activation energies, E_a and E_{α} , points a conduction occurring predominantly in band tails, with more density of states in the valence band, when compared to the conduction band. The difference $E_{\text{hop}} = E_a - E_{\alpha}$ is the hopping energy for holes or small polarons, also shown on Table 1, which is not very surprising since these materials are amorphous semiconductors, with no long range order. The values obtained for the hopping energies, between 0.08V and 0.25V, are typical for chalcogenide glasses [27]. In some samples it is very clear that the Seebeck coefficient presents a smooth maximum around 155 K, which is probably due to the transition to a

further localized variable range hopping conduction regime at lower temperatures [27]. The predicted temperature dependence, $\rho = \rho_0 \exp(A/T^{1/4})$, for the variable range hopping regime is not clearly observed at low temperatures, most probably because the change in regime occurs very smoothly and the temperature range of measurements was not wide enough.

The likely intrinsic semiconducting nature of the $\text{Cu}_{x+y}\text{Ge}_{20-x}\text{Te}_{80-y}$ glasses opens the possibility of further change their composition to optimize the electrical properties. Moreover, it should also allow the addition of glass stabilizing agents without degrading their electrical properties, in order to increase the glass transition temperatures and consequently their maximum temperature of application as thermoelectric materials and ZT values.

Conclusion

New chalcogenide glasses, with $\text{Cu}_{x+y}\text{Ge}_{20-x}\text{Te}_{80-y}$ ($0 \leq x \leq 20$; $0 \leq y \leq 10$) compositions, have been prepared by melt spinning and used to test the possibility of obtaining conducting glasses for thermoelectric applications. Their short-range order is most likely analogous to $\text{Ge}_{20}\text{Te}_{80}$ glasses, being based on CuTe_4 and GeTe_4 structural units. The addition of copper reduces the glass stability, but increases their thermoelectric properties, with a consequent huge increase on the power factor at $T = 300$ K, from $3.3 \times 10^{-3} \mu\text{W}/\text{K}^2\text{m}$ up to $60 \mu\text{W}/\text{K}^2\text{m}$ for the glasses with the extreme $\text{Ge}_{20}\text{Te}_{80}$ and $\text{Cu}_{27.5}\text{Ge}_{2.5}\text{Te}_{70}$ compositions, respectively. The exceptionally low thermal conductivity measured on the $\text{Ge}_{20}\text{Te}_{80}$ glass, together with the type of structural replacement and the low electrical contribution for the thermal conductivity point to a similar behavior on all series, definitely indicating the $\text{Cu}_{x+y}\text{Ge}_{20-x}\text{Te}_{80-y}$ -based glasses as having good potential for high performance thermoelectric materials. Their probable intrinsic semiconducting nature opens the possibility of further improvements, and clearly indicates conducting glasses as very promising thermoelectric materials.

ACKNOWLEDGMENT: This work was partially supported by FCT, Portugal, under the contract nr. PTDC/QUI/65369/2006, by the bi-lateral French-Portuguese exchange Program GRICES 2007-2008 and European COST P16 program.

FIGURE CAPTIONS

Figure 1. Ternary diagram Cu-Ge-Te showing the prepared compositions.

Figure 2. X-ray diffraction patterns of the $\text{Cu}_{x+y}\text{Ge}_{20-x}\text{Te}_{80-y}$ glasses (asterisks: tellurium; crosses: CuTe; circles: $\text{Cu}_{1.33}\text{Ge}_{0.57}\text{Te}_2$).

Figure 3. Photo of a $\text{Cu}_{22.5}\text{Ge}_{2.5}\text{Te}_{75}$ glass, including some crystallized part.

Figure 4. DSC measurements versus temperature showing glass transition (T_g) and crystallization temperatures (T_C) in $\text{Cu}_{20}\text{Te}_{80}$ and $\text{Cu}_{20}\text{Ge}_5\text{Te}_{75}$.

Figure 5. Variation of the room temperature resistivity of the $\text{Cu}_{x+y}\text{Ge}_{20-x}\text{Te}_{80-y}$ glasses as function of composition.

Figure 6. Electrical resistivity versus temperature in the Cu-Ge-Te glass system.

Figure 7. Variation of the room temperature Seebeck coefficient of the $\text{Cu}_{x+y}\text{Ge}_{20-x}\text{Te}_{80-y}$ glasses as function of composition.

Figure 8. Variation of the Seebeck coefficient of the $\text{Cu}_{x+y}\text{Ge}_{20-x}\text{Te}_{80-y}$ glasses versus temperature.

Figure 9. Variation of the room temperature power factor of the $\text{Cu}_{x+y}\text{Ge}_{20-x}\text{Te}_{80-y}$ glasses as function of composition.

TABLES.

Table 1. Electrical transport properties (ρ_{300K} , E_p , α_{300K} , E_α , E_{Hopp} and power factor parameters) of the $Ge_{20}Te_{80}$ -based glasses

Glass Composition	ρ_{300K} ($\mu\Omega m$)	$E_{p(High T)}$ (meV)	α_{300K} ($\mu V/K$)	$E_{\alpha(High T)}$ (meV)	E_{Hopp} (meV)	α^2/ρ ($\mu W/K^2m$)	Reference
$Ge_{20}Te_{80}$	2.8×10^8	470	960	-	-	3.3×10^{-3}	[9]
$Cu_7Ge_{13}Te_{80}$	5.8×10^6	340	505	84	256	4.4×10^{-2}	This work
$Cu_{7.5}Ge_{15}Te_{77.5}$	2.1×10^7	351	562	58	293	1.5×10^{-2}	This work
$Cu_{12}Ge_{12}Te_{76}$	1.2×10^6	298	361	-	-	1.1×10^{-1}	This work
$Cu_{15}Ge_{7.5}Te_{77.5}$	1.6×10^5	244	540	122	122	1.8	This work
$Cu_{20}Ge_5Te_{75}$	2.9×10^5	263	453	34	229	0.7	This work
$Cu_{22.5}Ge_{2.5}Te_{75}$	6×10^3	164	415	46	117	29	This work
$Cu_{27.5}Ge_{2.5}Te_{70}$	2.6×10^3	126	394	45	81	60	This work

REFERENCES

- [¹] Slack, G. *CRC Handbook of Thermoelectrics*; Rowe, D.M., Ed.; CRC Press: Boca Raton, FL, 1995.
- [²] Gonçalves, A.P.; Lopes, E.B.; Alves, E.; Barradas, N.P.; Franco, N.; Rouleau, O.; Godart, C. *NATO ASI Series B "Properties and Applications of Thermoelectric Materials"*; Zlatić, V., Hewson A., Eds.; Springer, 2009, submitted.
- [³] Godart, C.; Gonçalves, A.P.; Lopes, E.B.; Villeroy B. *NATO ASI Series B "Properties and Applications of Thermoelectric Materials"*; Zlatić, V., Hewson A., Eds.; Springer, 2009, accepted for publication.
- [⁴] Nolas, G.S.; Goldsmid, H.J. *Phys. Stat. Sol. (a)* **2002**, 194, 271-276.
- [⁵] Gonçalves, A.P.; Lopes, E.B.; Godart, C.; Alleno, E.; Rouleau, O. Portuguese Patent 103351, 2006.
- [⁶] Petersen, K.E.; Birkholz, U.; Adler, D. *Phys. Rev. B* **1973**, 8, 1453-1461.
- [⁷] Sidorov, V.A.; Brazhkin, V.V.; Khvostantsev, L.G.; Lyapin, A.G.; Sapelkin, A.V.; Tsiok, O.B. *Phys. Rev. Lett.* **1994**, 73, 3262-3265.
- [⁸] El-Oyoun, M.A. *J. Phys. D: Appl. Phys.* **2000**, 33, 2211-2217.
- [⁹] Parthasarathy, G.; Bandyopadhyay, A.K.; Asokan, S.; Gopal, E.S.R. *Solid State Commun.* **1984**, 51, 195-197.
- [¹⁰] Ferhat, A.; Ollitrault-Fichet, R.; Mastelaro, V.; Benazeth, S.; Rivet, J. *J. de Physique IV* **1992**, 2,C2-201-C2-206.
- [¹¹] Ramesh, K.; Asokan, S.; Sangunni, K.S.; Gopal, E.S.R. *Phys. Chem. Glasses* **1996**, 37, 217-220.

-
- [¹²] Almeida, M.; Oostra, S.; Alcácer L. *Phys. Rev. B* **1984**, *30*, 2839-2844.
- [¹³] Huebener, R.P. *Phys. Rev.* **1964**, *135*, A1281-A1291.
- [¹⁴] Lopes, E.B.; Almeida, M. *Physics Letters A* **1988**, *130*, 98-100.
- [¹⁵] Powers, R.W.; Ziegler J.B.; Johnston, H.L. Thermophysical properties of matter. Touloukian, Y.S., Powel, R.W., Ho C.Y., Klemens P.G., Eds.; Plenum: New York, 1970; Vol.1.
- [¹⁶] Kameda, Y.; Uemura, O.; Usuki, T. *Mater. Trans. JIM* **1996**, *37*, 1655-1658.
- [¹⁷] Kaban, I.; Halm, Th.; Hoyer, W.; Jóvári, P.; Neufeind, J. *J. Non-Cryst. Solids* **2003**, *326-327*, 120-124.
- [¹⁸] Hoyer, W.; Kaban, I.; Jóvári, P.; Dost, E. *J. Non-Cryst. Solids* **2004**, *338-340*, 565-568.
- [¹⁹] Casas-Ruiz, M.; Vásquez, J.; Ligeró, R.A.; Jiménez-Garay, R. *J. Mater. Science* **1993**, *28*, 1037-1044.
- [²⁰] Baranova, R.V.; Pinsker, Z.G. *Sov. Phys. Crystallogr.* **1964**, *9*, 83-85.
- [²¹] Kaban, I.; Dost, E.; Hoyer, W. *J. Alloys Compd.* **2004**, *379*, 166-170.
- [²²] Ramesh, K.; Asokan, S.; Sangunni, K.S.; Gopal, E.S.R. *J. Phys.: Condens. Matter* **1999**, *11*, 3897-3906.
- [²³] *CRC Handbook of Chemistry and Physics*; D.R. Lide, Ed.; Taylor and Francis: Boca Raton, FL, 2007.
- [²⁴] Sales, B.C.; Mandrus, D.; Williams, R.K. *Science* **1996**, *272*, 1325-1328.
- [²⁵] Mastronardi, K.; Young, D.; Wang, C.-C.; Ramirez, A.P.; Khalifah, P.; Cava, R.J. *Appl. Phys. Lett.* **1999**, *74*, 1415-1417.

[²⁶] Singh, A.K.; Kumar, P.; Singh, K.; Saxena, N.S. *Chalcogenide Letters* **2006**, 3, 139-144

[²⁷] Nagels, P. *Amorphous semiconductors*; Brodsky, M.H., Ed.; Springer Verlag: Berlin, 1985.

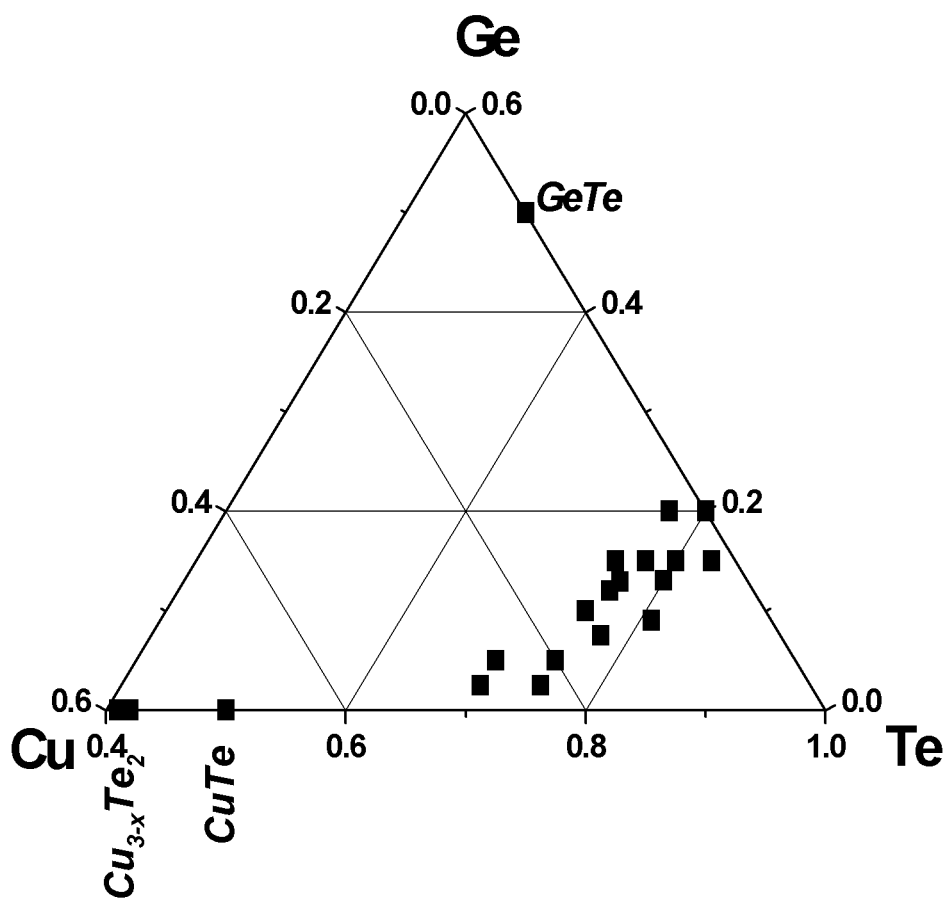


Figure 1

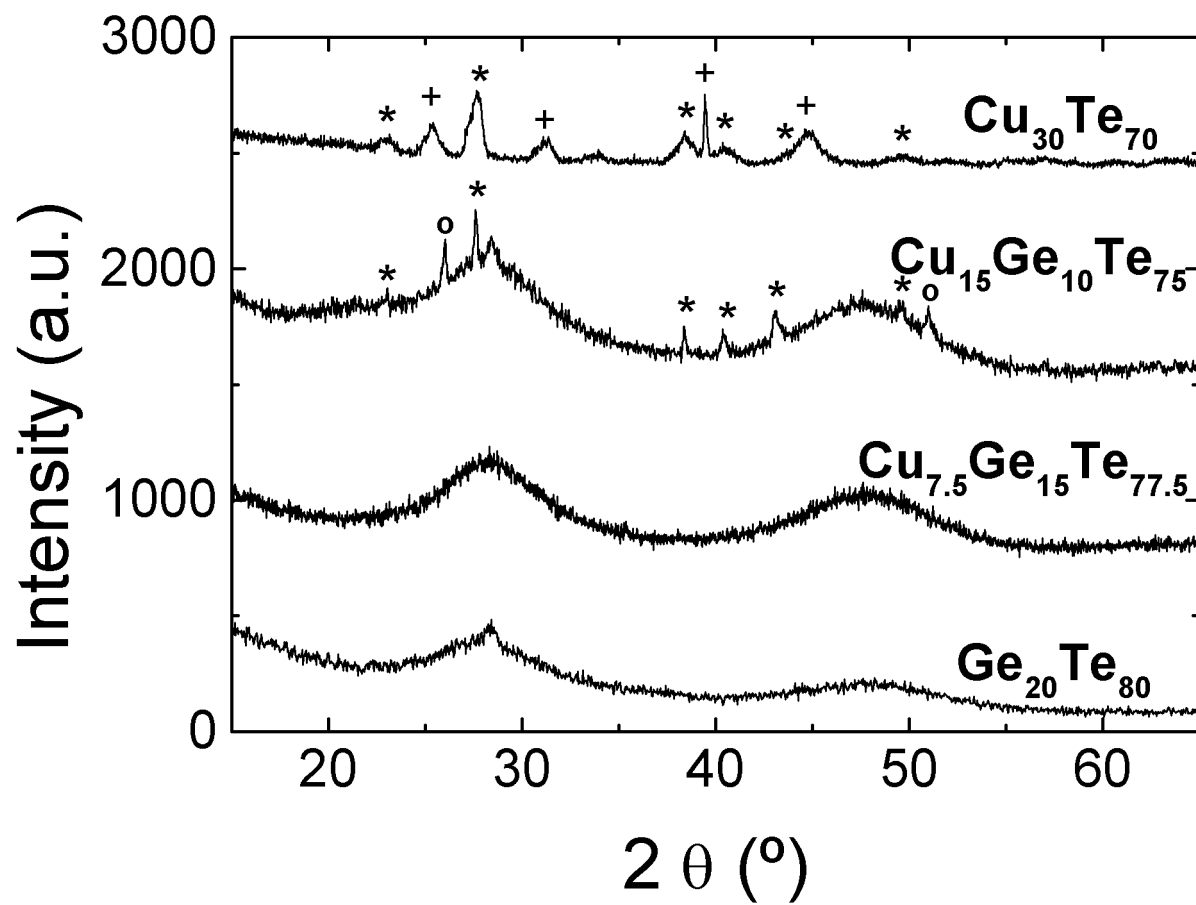


Figure 2

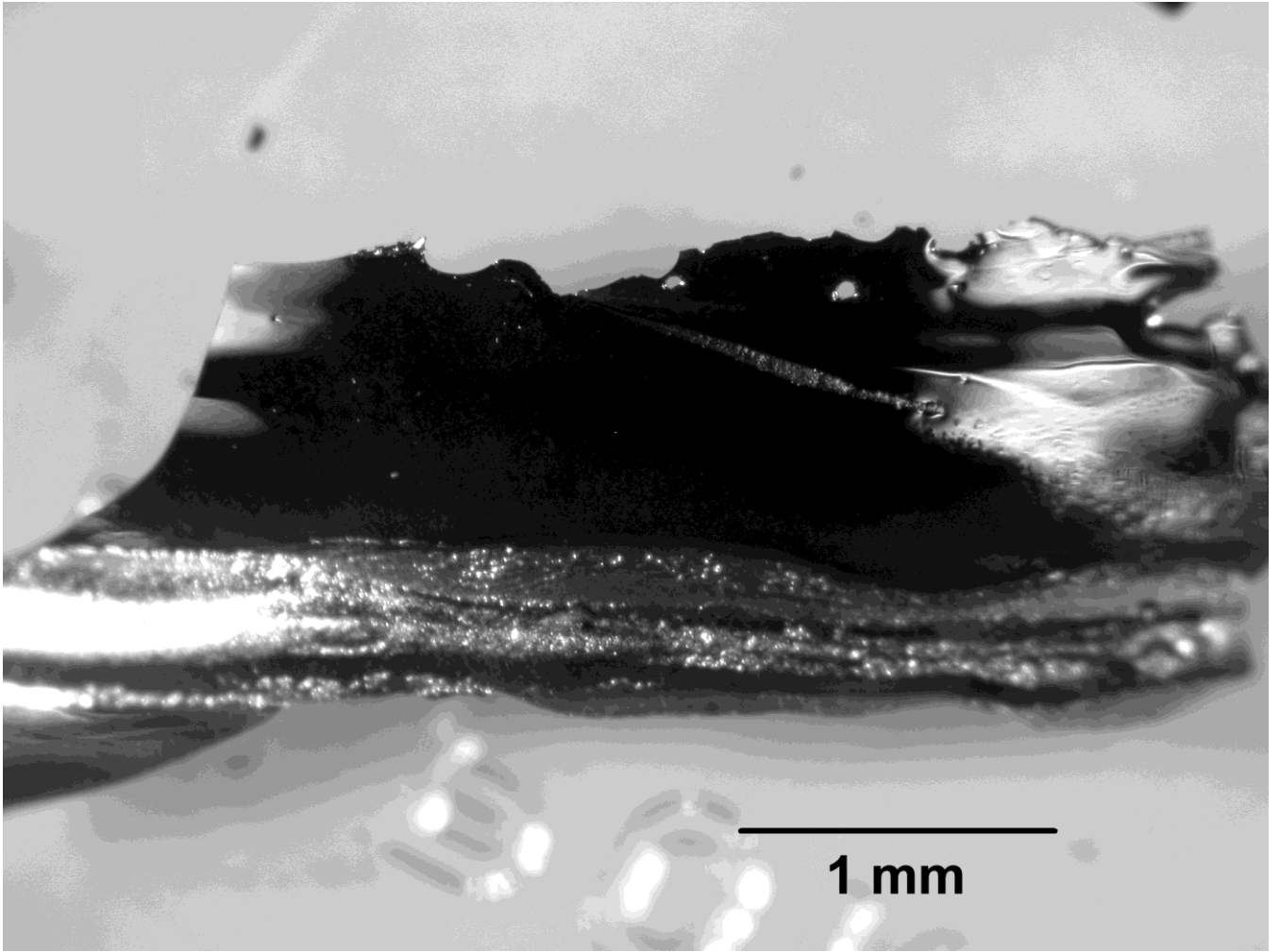


Figure 3

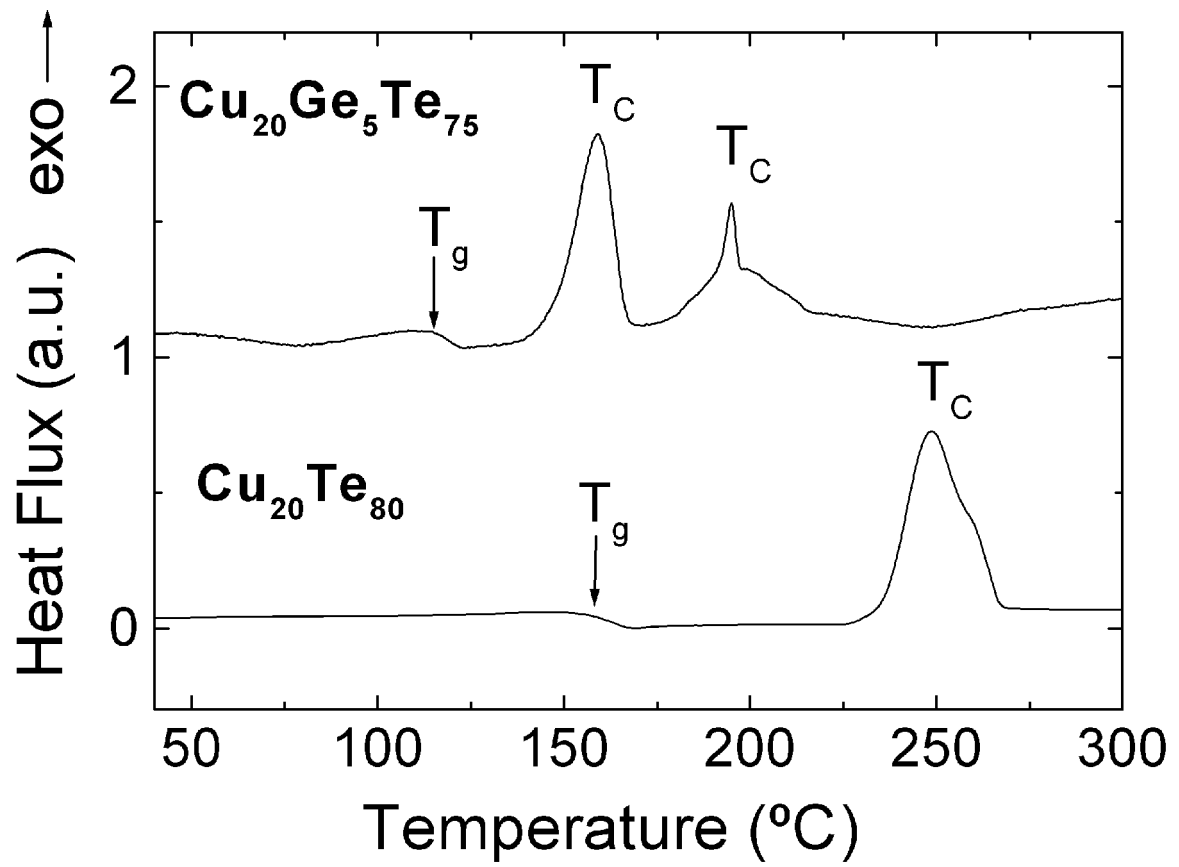


Figure 4

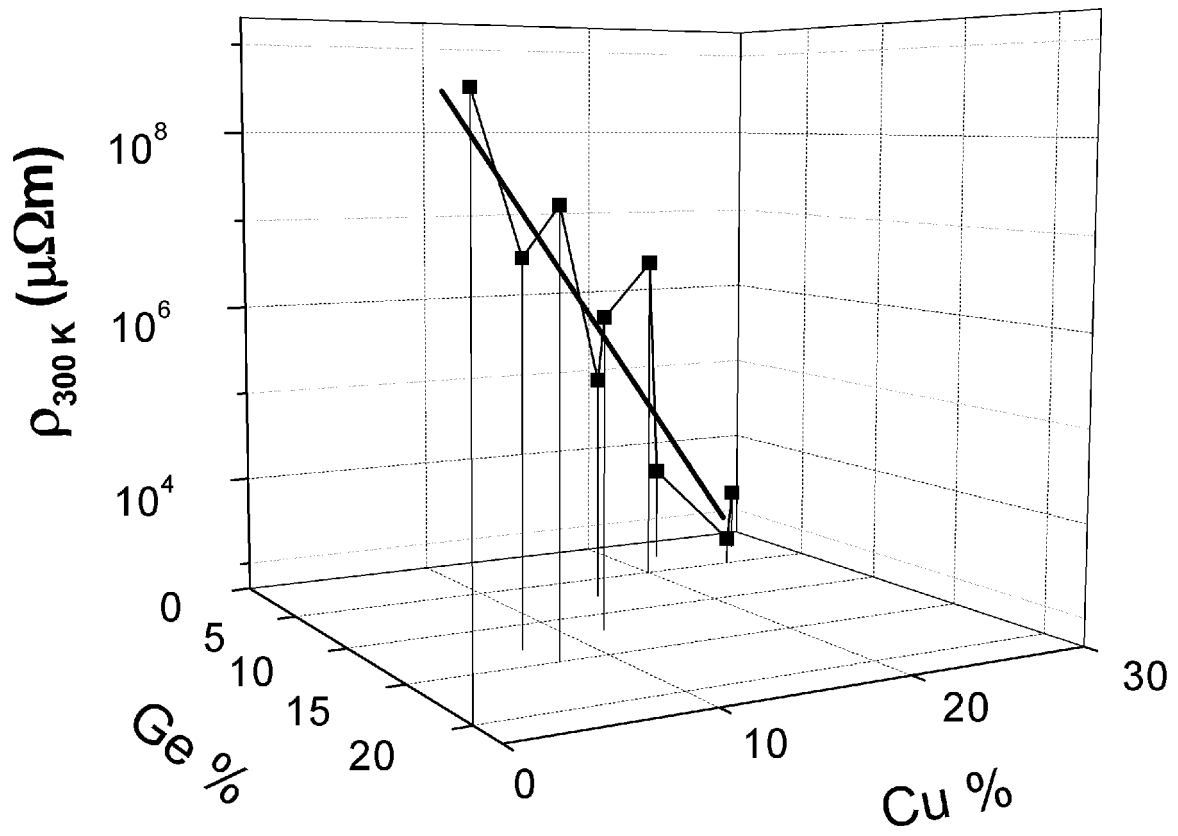


Figure 5

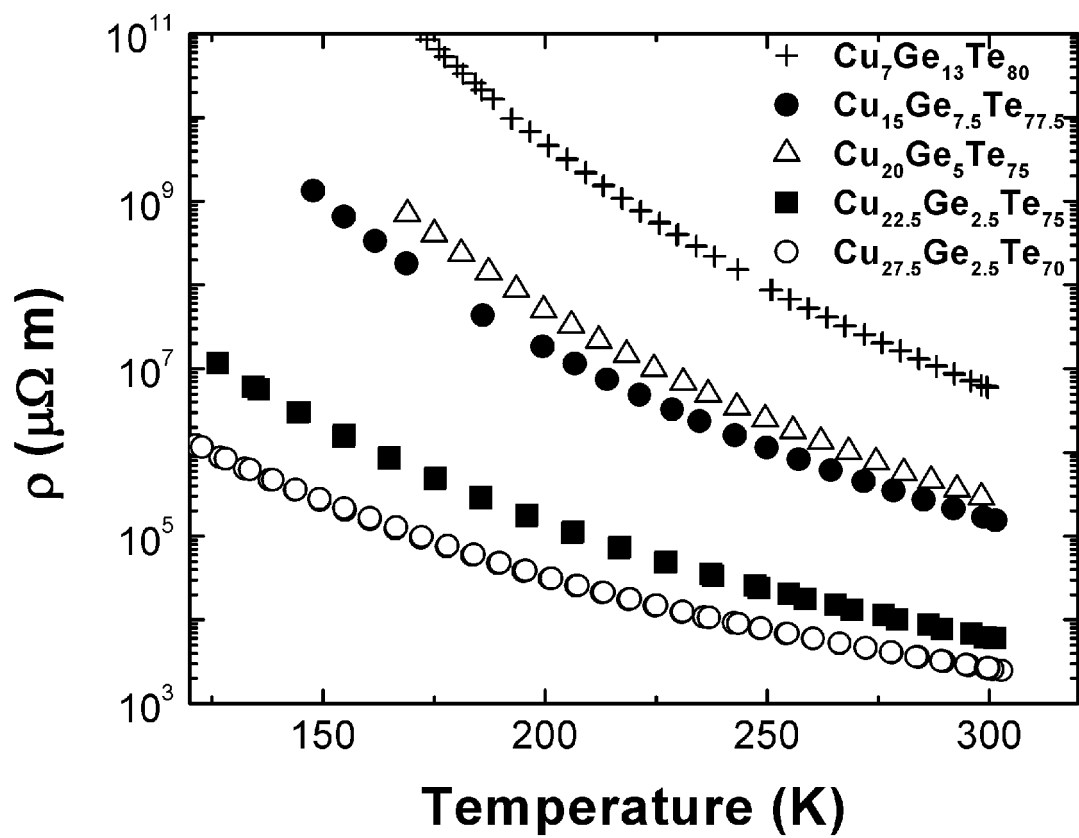


Figure 6

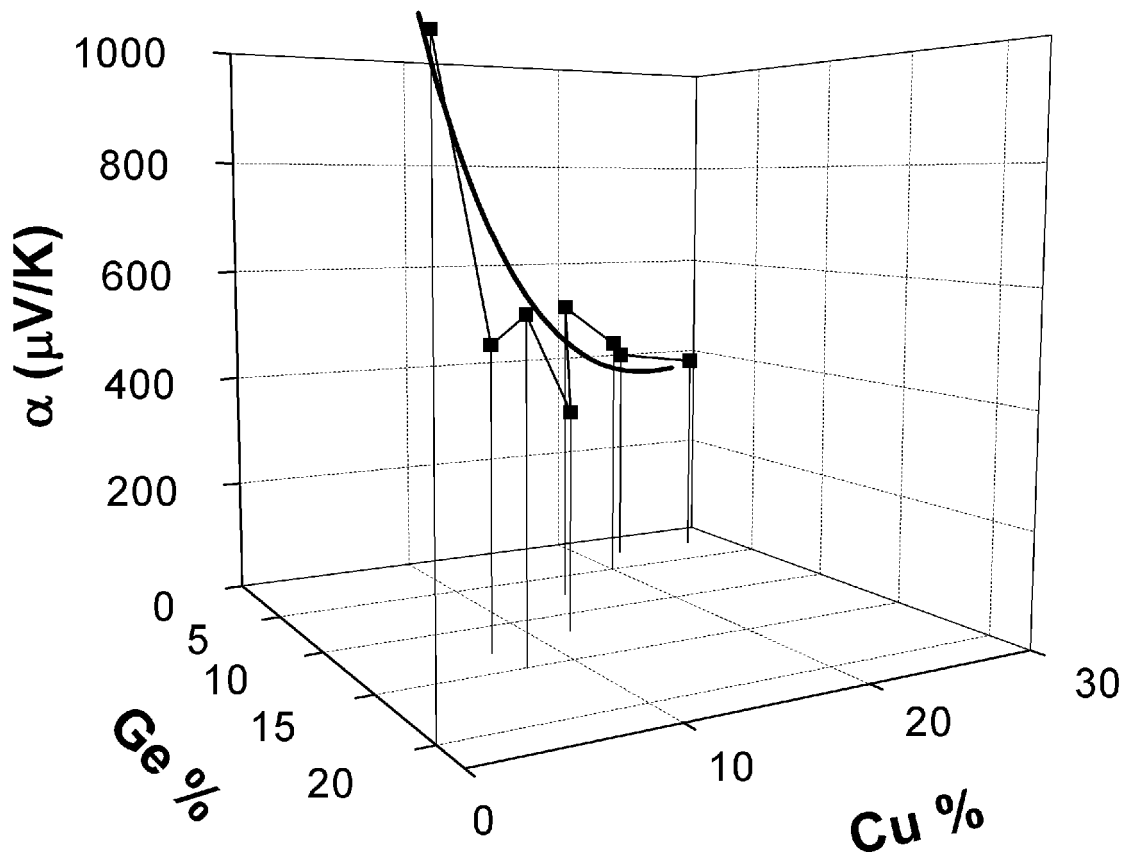


Figure 7

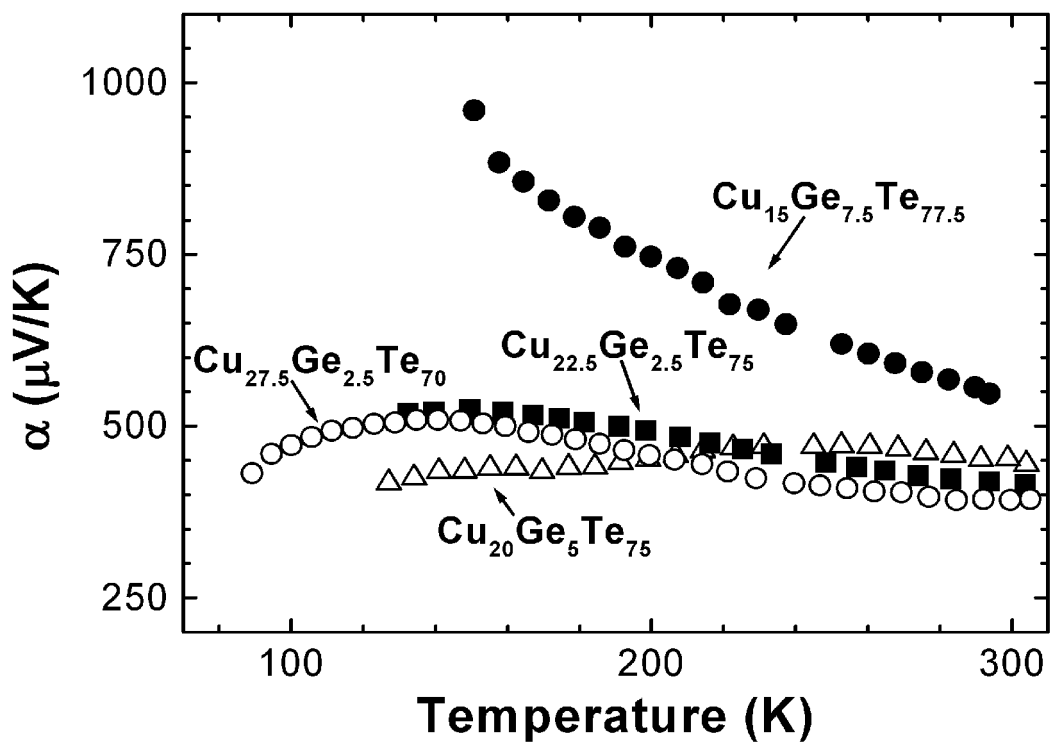


Figure 8

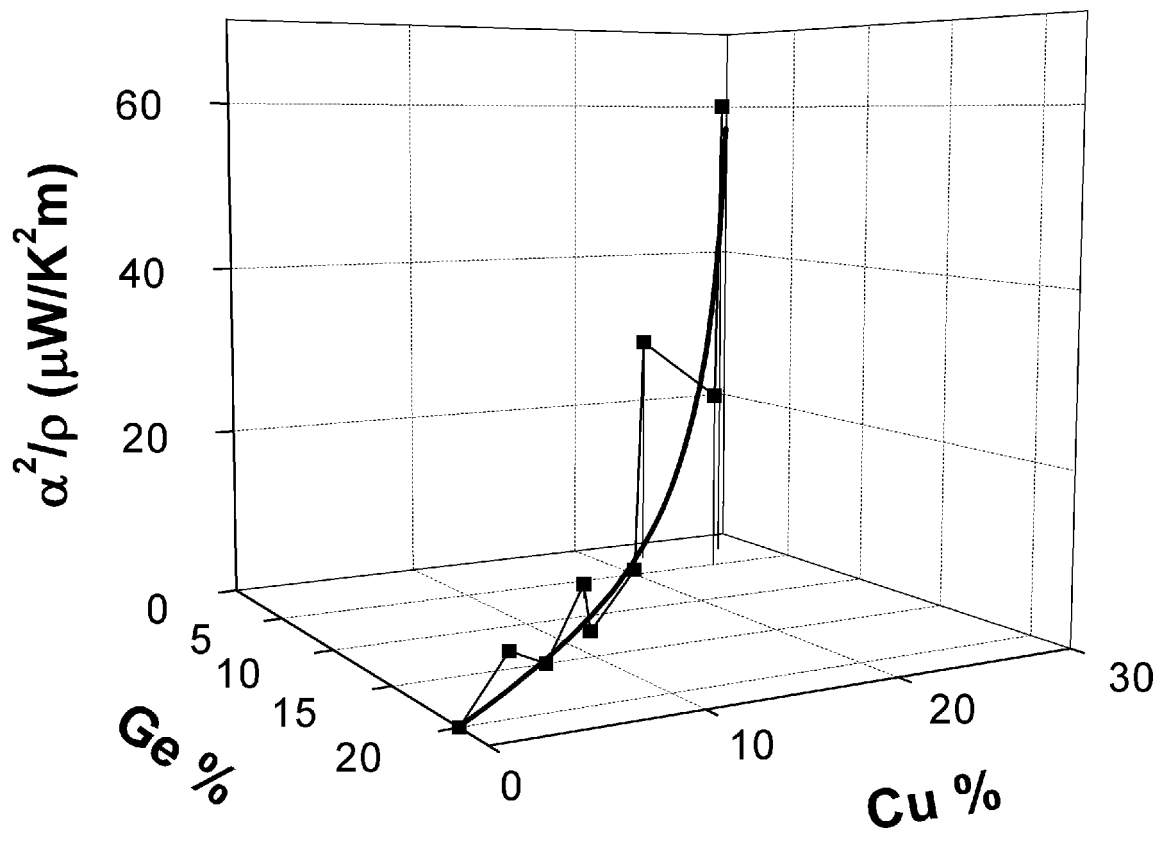


Figure 9